



FLOTATION OF BASTNAESITE ORE USING NOVEL COLLECTORS

D. Everly and C. Anderson

Kroll Institute for Extractive Metallurgy, Colorado School of Mines, Golden, CO

S. Jansone-Popova, V. Bryantsev, and B. Moyer

Oak Ridge National Laboratory, Chemical Sciences Division, Oak Ridge, TN

ABSTRACT

Interest in rare earth elements (REEs) has increased due to their distinct properties and new applications. China currently has a monopoly on rare earth production due to the lack of an economically viable process used outside of China. Bastnaesite, a rare earth fluorocarbonate, is one of the most common minerals containing REEs, which is mostly comprised of cerium and other light REEs. The objective of this research is to find a novel collector for the beneficiation of bastnaesite through froth flotation experiments to increase the grade and recovery of rare earth oxides while rejecting the major gangue minerals. Microflotation and rougher bench flotation studies were evaluated to find optimal collector(s) from 19 possible candidates. Collector 2, 5, and 8 were the top performing collectors chosen from microflotation experiments. A design of experiment matrix was set up to evaluate the variables, variable interactions, and provide a reference matrix for future optimization studies. Collector 2 was assessed to be the optimal collector. A rougher flotation experiment produced a rare earth oxide grade and recovery of 41% and 78%, respectively with a 91.5% rejection of calcite. Collector 8 and 14 also showed promising results to replace fatty acid.

KEYWORDS

Bastnaesite, Flotation, Microflotation, Rare earth elements

INTRODUCTION

Rare earth element (REE) production is important because they have broad and diverse applications in today's industry. China is the leading producer of rare earths with over 90% of the worldwide production. To avoid being dependent on China, the United States needs to find an economically viable process to produce REEs. The REEs include scandium, yttrium, and the light and heavy lanthanides. REEs are generally found together as rare earth oxides. Some common applications are: catalyst, phosphors, optics polishing media, magnets, batteries, and lasers. Finding suitable replacements for rare earths is difficult because of the strength, durability, and resistance to oxidation that they offer. The three largest reserves of rare earths are located in China, Brazil, and Russia according to a recent United States Geological Survey, and the world reserves total approximately 120 million metric tonnes of rare earth oxides (U.S. Geological Survey, 2017).

The ability to separate each element from the mineral and the desired mineral from the gangue minerals are major challenges that have been drawing a lot of attention in the past few decades. Bastnaesite is one of the most abundant minerals that contain REEs. Bastnaesite is a rare earth fluorocarbonate, and pure or concentrated samples contain up to 75% rare earth oxide, which contains approximately 50% cerium oxide. Bastnaesite minerals are found in vein deposits, contact metamorphic zones, and pegmatites (Gupta & Krishnamurthy, 2005). Barite, calcite, silicate, and dolomite are the major gangue minerals associated with bastnaesite, which have similar properties and behavior as bastnaesite. This drives the need to

understand surface chemistry using fundamental studies to find optimal conditions for selective adsorption of reagents and flotation of the desired mineral, bastnaesite.

Froth flotation is a method used to separate desired minerals from gangue minerals based on selective adsorption of reagents. The goal of flotation is to have the desired mineral in solution attach to an air or nitrogen bubble and form a froth layer, which is periodically scraped off and collected. Bastnaesite is a hydrophilic mineral so collectors are required to make the mineral hydrophobic. The hydrophobic minerals can then attach to the air bubbles and form a froth. It is important to find a collector that has selectivity for the desired mineral over gangue minerals to provide a good separation. Depressants can be used to coat certain mineral surfaces to inhibit adsorption of the collector on gangue minerals. No depressants are currently able to completely depress all gangue minerals; thus, collector selectivity is very important.

Collectors are organic electrolytes that can be either anionic or cationic, and they usually have a polar ionic function group that determines selectivity and a hydrocarbon tail that relates to collector solubility. Fatty acids, hydroxamic acids, and phosphoric acids have been used in the study of the beneficiation of bastnaesite. The major difference in these collector groups is the atom that the oxygen atoms are attached (carbon, nitrogen, and phosphorous; Jordens, Marion, Kuzmina, & Waters, 2014). The collectors currently used do not provide selectivity of bastnaesite over its gangue minerals; therefore, there is an incentive to find an ideal collector.

Fatty acids are frequently used because they are inexpensive and there has been extensive research done with them, but they require a lot of energy and reagents to get some selectivity. Hydroxamates have been researched as a replacement to fatty acids because they provide an increased selectivity of bastnaesite due to chelation. The mechanism for chelation precedes with the dissolution of the metal cation, hydrolysis of the cation, hydroxyl complex formation, and finally the re-adsorption of the hydroxyl complex on the mineral surface (Pradip & Fuerstenau, 1983, 1985). Chelation of a particle's surface may occur when the lattice atom is oriented such that the steric hinderance between ligand molecules is minimized during the bond formation step (Assis, Montenegro, & Peres, 1996).

Based on literature, collectors with aromatic hydroxamic acids and unsaturated groups are strong donors due to intramolecular hydrogen bonding. These were important factors when designing new collectors (Pradip, 1981). Hydroxamates have gained selectivity due to the substitution of a nitrogen atom for a carbon atom that is bound to the oxygen atom of the collector's functional group. This bond decreases electronegativity and creates a weaker interaction with metal cations. Because rare earth metal cations are one of the more stable classes of hydroxamate-metal complexes, the selectivity of REE over the gangue is increased. The gangue minerals do not make as stable of complexes so they do not bind as favorably with hydroxamates (Pradip, 1981; Anderson, 2015).

Phosphoric acids have been increasingly studied as flotation collectors because they form complexes with transition metals and alkaline earths such as cassiterite, chromite, and bastnaesite. Since the bonding atom is phosphorous, these collectors are less electronegative than carboxylic acids and hydroxamates. This allows the oxygen atom to more readily form complexes with metal cations (Jordens et al., 2014).

Since flotation is a complex process, other reagents are introduced such as depressants, pH modifiers, and/or frothing agents. Soda ash is used in flotation to adjust the pH of the pulp and control the carbonate equilibria. Sodium carbonate contributes to the absorption and charge at the mineral water interface due to it being a potential determining ion. Lignin sulphonate has been shown to effectively depress barite and partially calcite for both fatty acids and hydroxamate collectors (Pradip, 1981).

Research on the beneficiation of bastnaesite often includes both microflotation and bench scale flotation to study collector effects on the recovery of rare earths and rejection of gangue minerals. Calcite is a major problem in bastnaesite flotation because of the downstream acid consumption it requires. Microflotation is an important fundamental study because of the ability to control process variables and the

large number of tests that can be done in a short amount of time. Bench scale flotation is used to determine how the reagents affect flotation performance when the scale of flotation and slurry density is increased.

METHODS AND MATERIALS

The ore samples used in this flotation research were obtained from Mountain Pass Mine in California. All ore samples were jaw crushed, roll crushed, and separated into representative samples using a Jones Riffle. The mineralogy was determined by x-ray fluorescence (XRF) and mineral liberation analysis (MLA). The latter was performed by Montana Tech to find mineral composition and the optimal liberation of bastnaesite. Grinding times ranging from 0 to 90 minutes were analyzed at multiple size fractions. A 60-minute grinding period and -200x400 mesh size fraction were chosen for the microflotation experiments due to the high liberation and composition of bastnaesite in the ore as shown in Table 1. The P_{80} of the 60-minute size fraction was 50 μm , which is similar to the particle size used in industry for REO flotation. Although there was high liberation in the 90-minute and -400 mesh size fractions, they were not chosen because of the negative effect particles in this size fraction can have on flotation.

Table 1. Mineral composition of bastnaesite ore after a 60 minute grind period based on size fraction

Mineral	Formula	+100	100 X 200	200 X 400	-400	Modal
Barite	BaSO_4	7.29	10.2	20.9	33.8	27.3
Calcite	CaCO_3	11.8	21.5	20.8	17.6	19.0
Bastnaesite	$(\text{Ce}, \text{La})(\text{CO}_3)_2\text{F}$	2.99	4.12	10.7	12.8	11.3
Dolomite	$\text{CaMg}(\text{CO}_3)_2$	5.22	14.4	13.3	8.97	10.89
Quartz	SiO_2	4.28	12.6	9.84	5.14	7.38
K Feldspar	KAlSi_3O_8	4.19	11.4	7.35	4.02	5.81
Strontianite	SrCO_3	0.63	1.78	2.33	2.77	2.53
Paromite	$\text{Ca}(\text{Ce}, \text{La})_2(\text{CO}_3)_3\text{F}_2$	0.93	1.11	1.79	2.77	2.29
FeO	Fe_3O_4	9.76	2.73	2.19	2.18	2.25
Mica	$\text{KAl}_2(\text{AlSi}_3\text{O}_10)(\text{OH})_2$	1.43	5.57	2.68	1.41	2.21
Biotite	$\text{K}(\text{Mg}, \text{Fe})_3(\text{AlSi}_3\text{O}_10)(\text{OH})_2$	40.5	6.35	2.01	1.19	2.03
Monazite	$(\text{La}, \text{Ce})\text{PO}_4$	0.25	0.48	0.99	2.07	1.57
Celestine	SrSO_4	0.33	0.71	1.11	1.77	1.45
Ankerite	$\text{CaFe}(\text{CO}_3)_2$	4.12	2.05	1.02	1.32	1.30
Plagioclase	$(\text{Na}, \text{Ca})(\text{Al}, \text{Si})_4\text{O}_8$	0.85	2.21	1.47	0.66	1.07
Chlomite	$(\text{Mg}^2\text{Fe}^2)\text{Al}(\text{AlSi}_3\text{O}_10)(\text{OH})_8$	1.27	1.57	0.59	0.38	0.57
Apatite	$\text{Ca}_5(\text{PO}_4)_3\text{F}$	0.08	0.10	0.21	0.36	0.29
Hornblende	$(\text{Ca}_2\text{Na})(\text{Mg}^2\text{Fe}^2\text{Al})\text{Si}_6\text{O}_22(\text{OH})_2$	1.01	0.48	0.28	0.14	0.22
Allanite	$(\text{Ca}, \text{Ce})_2(\text{Al}, \text{Fe})_3(\text{SiO}_4)(\text{Si}_2\text{O}_7)\text{O}(\text{OH})$	2.75	0.28	0.10	0.25	0.21
Rutile	TiO_2	0.04	0.12	0.10	0.14	0.12
Galena	PbS	0.03	0.01	0.04	0.16	0.11
Magnetoplumbite	$\text{Pb}(\text{Fe}, \text{Mn})_2\text{O}_12$	0.01	0.04	0.04	0.06	0.05
Kaolinite	$\text{Al}_2\text{Si}_2\text{O}_5(\text{OH})_4$	0.04	0.11	0.07	0.02	0.04
Ilmenite	FeTiO_3	0.10	0.11	0.03	0.02	0.03
Pyrite	FeS_2	0.02	0.02	0.03	0.01	0.02
Pyroxene	$\text{CaMgSi}_2\text{O}_6$	0.05	0.06	0.02	P	0.01
Zircon	ZrSiO_4	P	0.01	P	0.02	0.01
Thorite	ThSiO_4	ND	ND	0.01	0.01	0.01
Enargite Tenn	Cu_3AsS_4	ND	P	P	P	P
Plumbophyllite	$\text{Pb}_2\text{Si}_4\text{O}_{10} \cdot \text{H}_2\text{O}$	0.01	P	P	P	P

The material used for bench flotation was ground using a higher-powered roll crusher to obtain larger quantities of material. The product was ground for 45 minutes then wet sieved to 100% passing 100 mesh. The slurry was then filtered and dried. A particle size analysis was done on this product. The ground ore was wet-sieved through a 325-mesh screen. Both size fractions were then collected and dried. The +325-mesh sample was then run through a dry rotap for 25 minutes using 100, 115, 150, 200, 270, and 325 mesh screens. The material and each fraction was dried and weighed. The P_{80} of the ground material was approximately 50 μm .

X-ray fluorescence was used to measure the elemental compositions of the ore, flotation concentrates, and flotation tails. A method was set up using the XRF software to obtain a multivariable regression fit line based on standards with known compositions. The compositions of the elements in the ore were then fit to each of the corresponding regressions and converted from elemental composition to oxide composition. The REO compositions were determined from the cerium content since it provided the most consistent rare earth contents compared to Molycorp data. The cerium oxide content makes up 49.1% of the rare earth oxide content in the Mountain Pass ore deposit. The ore samples were fused into discs using a Katanax K1 Prime Fluxer. The discs were made using 2% sample and 98% lithium borate flux. The fusion discs allowed for a consistent and uniform sample without mineralogical effects to be analyzed by the XRF. The XRF results for the materials used in the fundamental studies and bench flotation are shown in Table 2. These results are consistent with Molycorp data, which had a head grade of approximately 8% REO.

Table 2. XRF oxide composition for microflotation (-200x400 mesh) and bench flotation (-100 mesh)

Fundamental Studies Material		Bench Flotation
Mineral	Composition (%)	Composition (%)
REO	7.70	8.01
CaO	16.29	16.91
BaO	12.61	13.72
SiO ₂	14.81	12.97

The 19 collectors used in this research were obtained from Oak Ridge National Laboratory. The collectors were labeled 1 through 18 and the tall oil was labeled as fatty acid. Those collectors that were not water soluble were dissolved in ethanol then emulsified in the ore slurry. Table 3 lists the collectors tested. Table 4 lists the other reagents used in this research.

Table 3. Reagent chemical structure, name, and CAS#

#	Chemical Structure	IUPAC Name	CAS#
1		N-hydroxybenzamide	495-18-1
2		N,2-dihydroxybenzamide	<u>89-73-6</u>
3		N1,N10-dihydroxydecanediamide	5578-84-7
4		4-(tert-butyl)-N-hydroxybenzamide	62034-73-5
5		N-hydroxycyclohexanecarboxamide potassium salt	13810-02-1 (N-hydroxycyclohexane carboxamide)
6		N-hydroxyoctanamide	7377-03-9
7		2-(4-butoxyphenyl)-N-hydroxyacetamide	

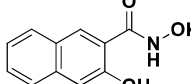
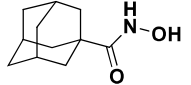
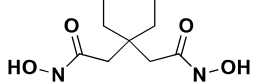
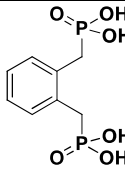
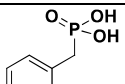
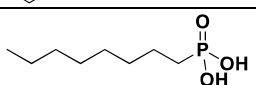
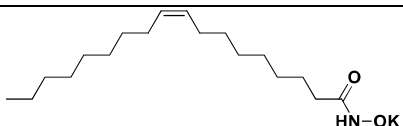
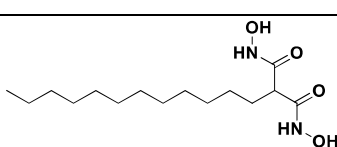
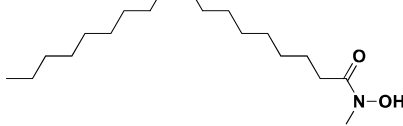
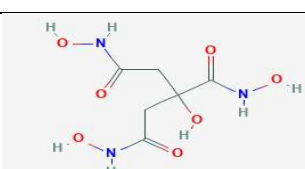
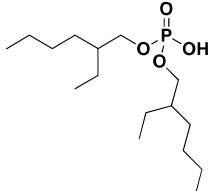
#	Chemical Structure	IUPAC Name	CAS#
8		N,3-dihydroxy-2-naphthamide potassium salt	22974-74-9 (N,3-dihydroxy-2-naphthamide)
9		(3r,5r,7r)-N-hydroxyadamantane-1-carboxamide	
10		2,2'-(cyclohexane-1,1-diyl)bis(N-hydroxyacetamide)	
11		(1,2-phenylenebis(methylene))bis(phosphonic acid)	42104-58-5
12		benzylphosphonic acid	6881-57-8
13		octylphosphonic acid	4724-48-5
14		N-hydroxyoleamide potassium salt	10335-69-0 (N-hydroxyoleamide)
15		2-dodecyl-N1,N3-dihydroxymalonamide	
16		N-hydroxy-N-methyloleamide	
17		2-(dodecyloxy)-N1,N2,N3-trihydroxypropane-1,2,3-tricarboxamide	405.49
18		bis(2-ethylhexyl) hydrogen phosphate	298-07-7

Table 4. Reagent type, name, and chemical formula

Type	Name	Chemical Formula
Depressant	Ammonium Ligno Sulfonate	C ₂₀ H ₁₇ O ₁₀ S ₂ (Lignin Sulphonate)
Frother	Methyl Iso-Butyl Carbonyl	C ₆ H ₁₄ O
Depressant	Sodium Carbonate	Na ₂ CO ₃
pH modifier	Hydrochloric Acid	HCl
pH modifier	Potassium Hydroxide	KOH
Ore	Bastnaesite	(Ce, La)(CO ₃)F
Flux	Lithium Borates	66.67% Li ₂ B ₄ O ₇ , 32.83% LiBO ₂ , 0.5% LiBr
Collector	Tall Oil	C ₁₈ H ₃₃ NaO ₂ (Sodium Oleate)
Solvent	Ethanol	C ₂ H ₆ O

Bastnaesite ore was used for all the microflotation experiments. A Partridge Smith Cell was used for the microflotation experiments. A 52-mL solution was made up with 1% ore, collector, pH modifier, and frother. The experiments were conducted of variable pH (8-11) and collector concentration. The ore was added to distilled water then placed on a stir plate. The pH was adjusted and maintained through the 15-minute conditioning stage. The dissolved collector was added to the slurry once the pH was set. Non-water-soluble collectors were dissolved in ethanol then emulsified by ultrasonication for three minutes before conditioning. One drop of frother was added to each experiment with 2 minutes remaining in the conditioning period. After the conditioning stage, 10 mL of the supernatant was extracted. The slurry was added to the microflotation cell then the beaker was rinsed with the extracted supernatant into the cell to prevent loss of material. A stir bar was added to agitate the solution. Compressed air was then introduced to the cell at a flow rate of 26.6 cm³/min. No heat, depressant, or pure minerals were used for the microflotation experiments to ensure selectivity was from the collector. The concentrates and tails were both filtered and dried. The experiments were done in duplicate then the respective concentrates and tails were combined to get enough sample to be fused into discs. The discs were then analyzed on the XRF.

A Metso Denver D-12 Legacy cell was used to conduct each experiment. A cell was used with 1L of distilled water and 25 wt% solids. A screening test was conducted using the Stat-Ease software to test the variables listed in Table 5.

Table 5. Bench flotation variables

Variable	Range
Collector	Collector 2, 5, 6, 8, 14, fatty acid
pH	8.5, 9.5, 10.5
Temperature (Celsius)	Ambient, 50, 81
Collector Concentration (g collector/kg ore)	High-Low (based on microflotation results)
pH adjustor	Soda Ash, KOH, HCl
Depressant Concentration (M)	0, 0.75, 1.5
Continued pH adjustment	No, Yes

For each experiment, the temperature of the slurry was adjusted before conditioning. Once the pH was adjusted, the depressant was added and followed by a five-minute conditioning period. This five-minute period was bypassed for tests not requiring a depressant. The collector was then added to solution for 10 minutes. Non-water-soluble collectors were dissolved in ethanol then emulsified by a Hamilton Beach Commercial HMI200 Immersion Blender for three minutes. The conditioning was done at 900 rpm rotor speed. 1 drop of frother was added to each experiment except with fatty acid as it hindered froth formation. A 4-minute flotation step was performed after the conditioning stage. The concentrates and tails were pressure filtered, dried, fused into discs, and analyzed with the XRF.

RESULTS AND DISCUSSION

Microflotation was used to screen the 19 collector candidates to find three candidates that had the highest selectivity and recovery of bastnaesite over the gangue minerals: calcite, barite, and silicate. Figure 1 shows the results for the optimal condition of each collector. Multiple tests were initially run for each collector to find a concentration range that would float approximately a third of the ore, half of the ore, and two-thirds of the ore. Although this graph only shows the best condition, each collector was run at nine different conditions with pH and/or collector concentration being adjusted.

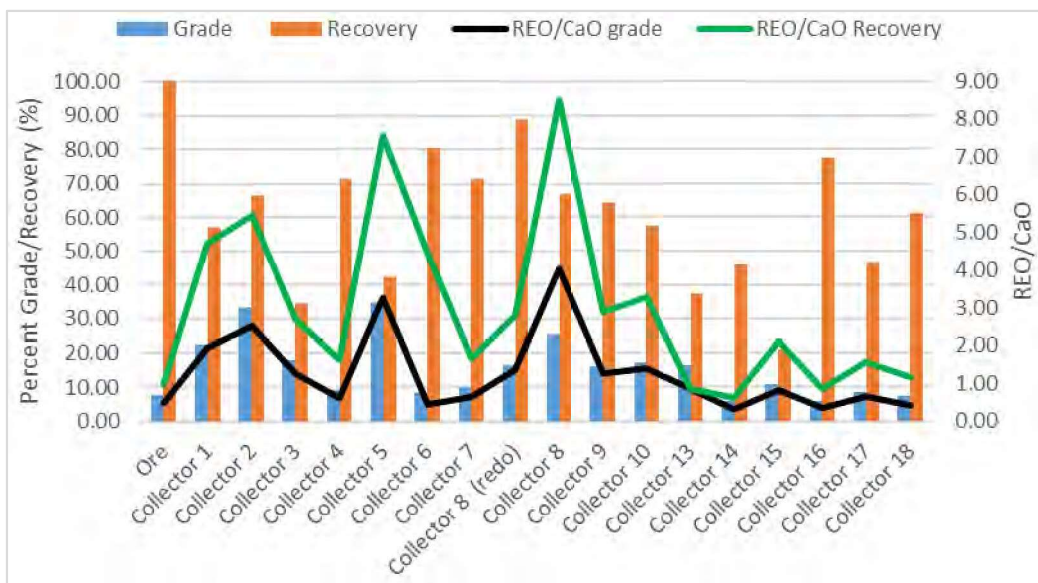


Figure 1. The primary axis compares the grade (blue) and recovery (orange) percentages versus the collector type. The secondary axis compares the ratio of REO to CaO grade (black) and recovery (green) to the collector type.

Collector 11 and 12 were not included in this figure because no condition tested was able to produce enough flotation concentrate to be analyzed. Fatty acid microflotation was also unsuccessful in producing a froth unless an unreasonable high concentration was used compared to the charge required for bench flotation. This may be attributed to the low slurry density used for microflotation. The frother used for every other collector could not be used for fatty acid because it destabilized the froth.

In the figure above, collector 8 had the best rejection of calcite and a higher REO grade and recovery. This collector was run twice because only two of the nine conditions tested showed selectivity. The result showed the same trend but was not fully repeatable. Collector 8 was still chosen to move on to bench flotation based on the promising results.

The microflotation results show collector 1, 2, 5, and 8 to have the highest increase in grade in the concentrate from the head grade of the ore. Collector 2 and 5 produced a rare earth oxide grade of approximately 33% and 35%, respectively. Although the respective REO recoveries were not very high, some other conditions tested by each collector were able to achieve high recoveries and only suffered slightly lower grades. The collectors that did not produce a significant increase in grade compared to the head grade were excluded from the potential top performing candidates.

Collectors 2, 5, and 8 had the highest rejection of calcite, which was a major factor because of the downstream costs. They also provided very good rejection of barite and silicate. From the REO grade, REO recovery, and gangue rejection, collectors 2, 5 and 8 were chosen for bench flotation experiments. Collector

6 and fatty acid were also selected for further testing as a comparison to previous research. Collector 14 was chosen due to its similarity of structure to oleic acid. Figure 2 shows the REO grade and recovery for each experimental condition for collectors 2, 5 and 8. The secondary axis depicts the ratios of REO to the gangue. From this graph, the trends are shown for each collector. Collector 2 and 5 show the best selectivity at lower pH values; collector 8 shows the flotation is very dependent on collector concentration and pH.

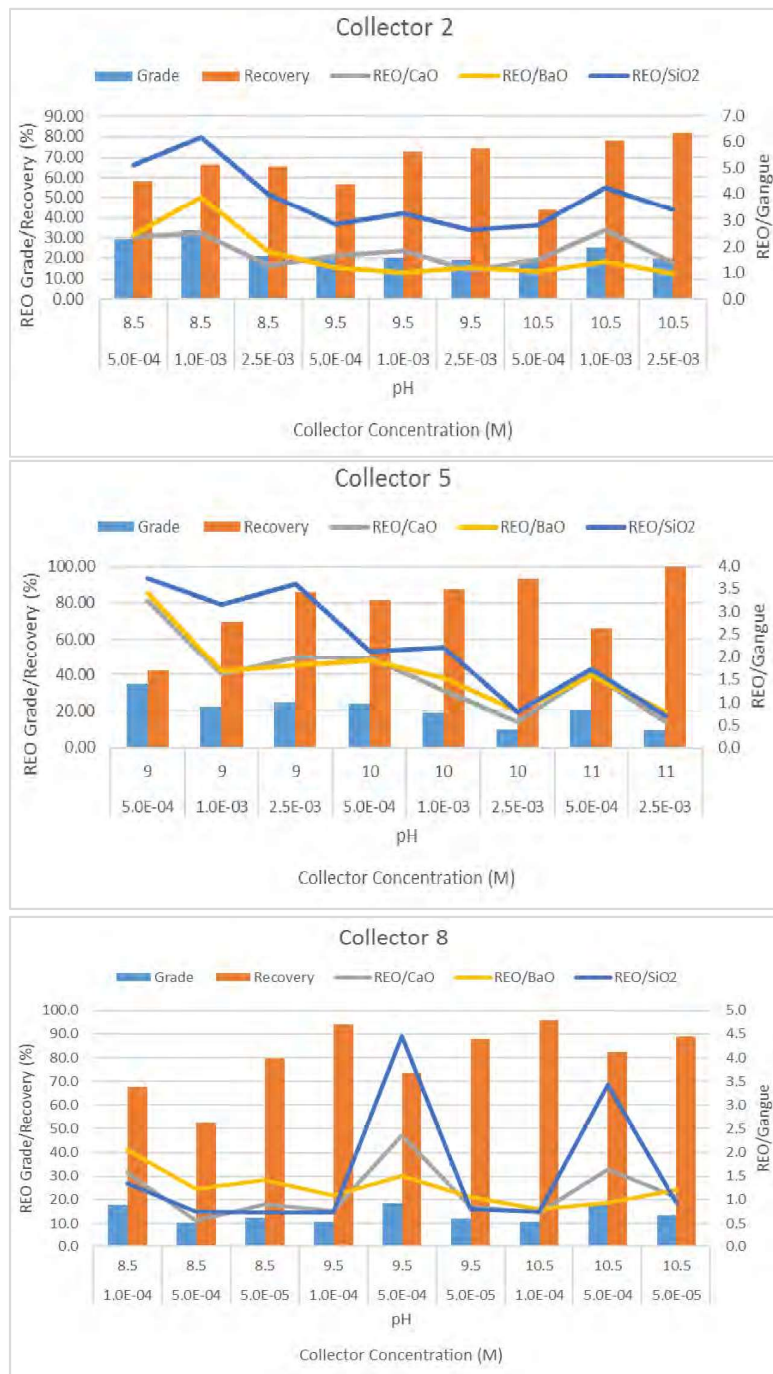


Figure 2. Grade/recovery and gangue rejection ratios versus the corresponding pH and collector concentration for collector 2 (top), collector 5 (middle), and the average of the collector 8 runs (bottom)

Rougher bench flotation was done using the six collectors described above. Two groups of flotation experiments were performed: a screening test and initial tests to get a frame of reference for the flotation variables. The variables included in the experiment were collector type, collector concentration (low, high), depressant concentration (0-1.5 mM), heat addition (RT-82°C), pH (8.5-10.5), pH modifier (KOH, soda ash), and whether the pH modifier was added continuously throughout the experiment or just initially. The screening matrix was set up using the Design Experiment 10 developed by Stat-Ease to determine the significant factors and interactions for each response. The four responses chosen were REO grade (%), CaO grade (%), BaO grade (%), and REO recovery (%). The design of experiment matrix included: factorial screening design, categoric factors, 50 randomized runs, 40 model points, and 10 residuals (5 lack of fit, 5 replicate). The number of runs was chosen to get a power value over 80% for each variable. Once all the experimental data were entered into the Stat-Ease software, grade and recovery outputs were examined to get a visual look at each response as shown in Figure 3.

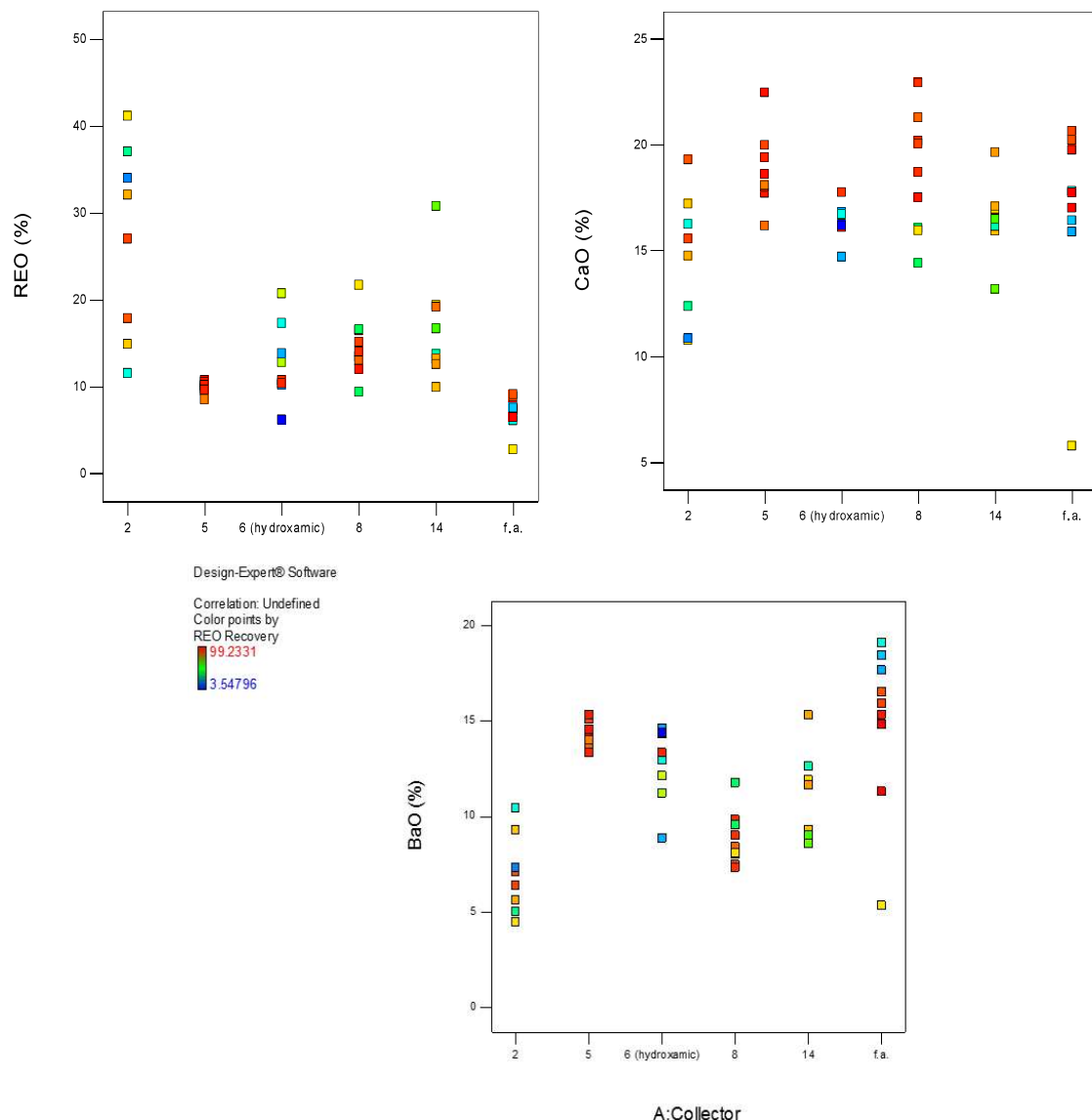


Figure 3. Grade percentage and REO recovery percentage versus collector type. The color represents the REO recovery percentage corresponding to the color shown in the top left corner of each graph.

The grades of REO, CaO, and BaO in the head grade ore are approximately 8%, 17%, and 14%, respectively. The graphs show that collector 2 produced the most promising and consistent results for each of the responses.

To determine the significant factors and interactions for the variables, Half-Normal plots were developed for each response. Using the ANOVA statistical analysis and Box-Cox plots for power transformations, the factors and interactions included in the half-normal plot were chosen to optimize the models shown in Figure 4.

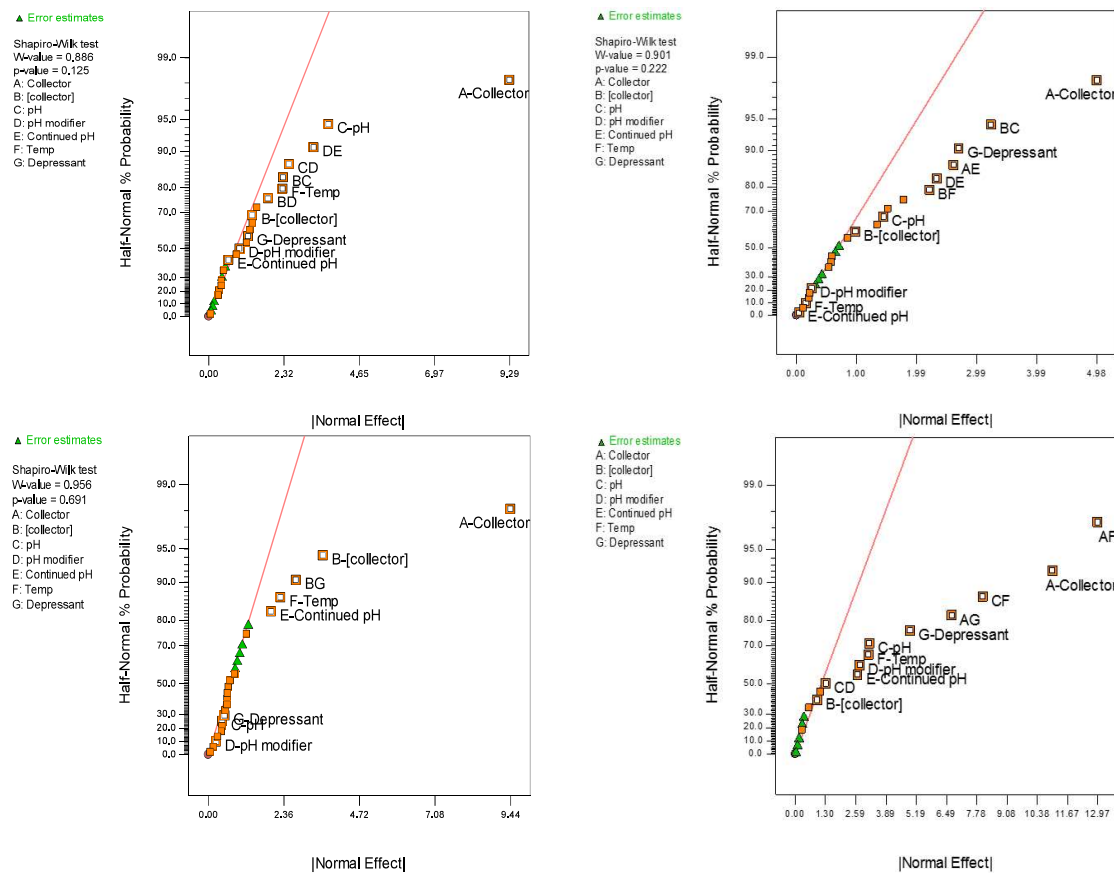


Figure 4. Half-Normal plots for REO grade (top left), CaO grade (top right), BaO grade (bottom left), and REO recovery (bottom right) in the concentrate.

The models were determined to be significant based on the model F-value, which describes if the error could be due to noise. The p-value was analyzed for each model and factor/interaction included in the model. The Half-Normal plot allows separation of effects into large and small effects. The large effects (usually to the right of the graph and red line) are likely to be repeatable effects; the small effects (lower left corner of graph) are likely to be caused by noise. The significant model factors and interactions are shown in Table 6 for each response.

Table 6. Significant model factors

Response	Significant Model Terms
REO Grade (%)	Collector type, pH, Temperature, Collector conc.-pH, pH-pH modifier, pH modifier-Cont. pH
BaO Grade (%)	Collector type, Collector conc., Temperature, Collector conc.-Depressant conc.
CaO Grade (%)	Collector type, Depressant conc., Collector type-Cont. pH, Collector conc.-pH, Collector conc.-Temperature, pH modifier-Cont. pH
REO Recovery (%)	Collector type, pH, pH modifier, Temperature, Depressant conc., Collector type-Temperature, Collector type-Depressant conc., pH-Temperature

Once the model was determined significant, the model graphs were used to look at the different factors and interactions for each of the responses. It might be difficult to compare which overall collector concentration was best between collectors since each collector requires a different optimum concentration. From the model graphs, there was a large variability between which reagent scheme worked best for each of the responses. This proves how complex froth flotation is and how hard it can be to find optimal flotation conditions. The design of experiment software also generated an optimization study from the chosen variable parameters. It predicted a further increase in grade, recovery, and gangue rejection, which is feasible due to the limited number of runs completed for each collector.

Figure 5 shows the optimal rougher bench flotation condition for each of the collectors. Data from the initial test work is included along with the data from the DOE matrix. The figure also shows the estimated flotation conditions from flotation experiments done by Molycorp. From this graph, collector 2 shows a significant increase in REO grade, REO recovery, and calcite rejection compared to the rest of the collectors tested and results from industry. Collectors 8 and 14 also exhibit promise as possible replacements to fatty acid flotation because of the increased rare earth recovery, calcite rejection, and they did not require heat addition.

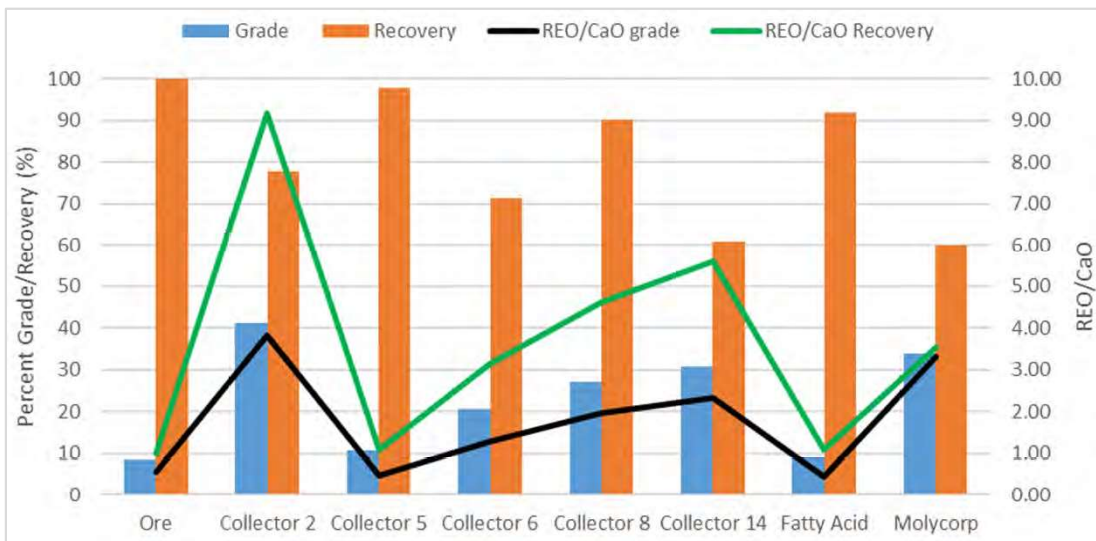


Figure 5. Grade/recovery and REO upgrade ratio to calcite versus collector type for the optimal flotation conditions for each collector

Collector 5 was tested at variable concentrations, but no selectivity of bastnaesite or increase in REO grade/recovery was exhibited compared to the promising results from microflotation experiments. Fatty acid did not produce expected results. This may result from the limited and randomized flotation conditions since fatty acid has shown in previous literature to only gain selectivity at high temperature and depressant

additions. Other possible explanations could be due to a different composition of tall oil (low rosin content) or lower slurry density.

MLA analysis was done on the flotation concentrates of collectors 2, 5, and 8. The sample was chosen based on the conditions that provided the best flotation performance. The mineralogy is shown in Table 7 for each of the collectors. The MLA analysis found the liberation of bastnaesite was 72% for collector 2 and 14 and 66% for collector 8. Bastnaesite accounted for approximately 80% of the cerium content with parsite and monazite accounting for the rest. Based on these MLA results, the unliberated particles may attribute to the gangue minerals in the flotation concentrate. Increasing the liberation of the ore without grinding to a size that would inhibit flotation could increase the rejection of gangue minerals and collector selectivity. Full rejection of calcium may not be possible as parsite and dolomite are significant sources in the flotation concentrates. There is still room for collector selectivity and process improvement as there is at least 11% calcite in the concentrates, which needs to be removed.

Table 7. MLA Modal Mineral Content for the flotation concentrates of the selected collectors

Mineral	Formula	C2	C8.7	C14
Bastnaesite	(Ce0.6La0.3Nd0.1)(CO3)F	48.5	34.2	40.7
Calcite	CaCO ₃	11.0	12.4	14.2
Parosite	Ca(Ce0.6,La0.3Nd0.1)2(CO3)3F2	10.7	9.68	7.28
Barite	BaSO ₄	5.62	9.38	11.4
Dolomite	CaMg(CO ₃) ₂	3.80	3.75	7.19
Monazite	(La,Ce)PO4	5.15	4.43	3.69
Strontianite	SrCO ₃	3.58	4.49	2.96
FeO	Fe ₂ O ₃	2.15	3.48	1.98
Quartz	SiO ₂	1.80	3.18	2.47
Ankerite	CaFe(CO ₃) ₂	1.42	4.04	1.38
K_Feldspar	KAlSi ₃ O ₈	1.04	2.55	1.61
Allanite	(Ca,Ce0.7,La0.2,Nd0.1)2(Al,Fe)3(SiO4)(Si₂O₇)O(OH)	0.77	1.74	0.34
Celestine_Ba	Sr _{0.65} Ba _{0.35} SO ₄	0.71	0.86	1.22
Hornblende	(Ca ₂ ,Na)(Mg ₂ FeAl)Si ₆ O ₂₂ (OH) ₂	0.46	1.33	0.66
Ancylite	Sr(Ce,La)(CO3)2(OH) . H₂O	0.62	1.01	0.26
Apatite	Ca ₅ (PO ₄) ₃ F	0.71	0.24	0.38
Chlorite	(Mg ₃ ,Fe ₂)Al(AlSi ₃)O ₁₀ (OH) ₈	0.26	0.49	0.32
Pyx_Amph	(CaMgSi ₂ O ₆)(Ca ₂ ,Na)(Mg ₂ FeAl)Si ₆ O ₂₂ (OH) ₂	0.24	0.31	0.26
Muscovite	KAl ₂ (AlSi ₃ O ₁₀)(OH) ₂	0.21	0.28	0.30
Rutile	TiO ₂	0.29	0.31	0.19
Anglesite	PbSO ₄	0.19	0.30	0.20
Ferroan_Magnesite	(MgFe)CO ₃	0.12	0.27	0.16
Galena	PbS	0.08	0.14	0.22
Coronadite	PbMn ₈ O ₁₆	0.09	0.20	0.06
Plagioclase	(Na,Ca)(Al,Si)4O ₈	0.04	0.18	0.07
Pyrite	FeS ₂	0.07	0.12	0.06
Ilmenite	FeTiO ₃	0.08	0.07	0.08
Hollandite	BaMn ₈ O ₁₆	0.03	0.10	0.04
Aegirine	NaFeSi ₂ O ₆	0.05	0.07	0.05
Andradite	Ca ₃ Fe ₂ (SiO ₄) ₃	0.03	0.11	0.04
Epidote	Ca ₂ (Al,Fe)3Si ₃ O ₁₂ OH	0.02	0.07	0.06
Svanbergite	SrAl ₃ (PO ₄)(SO ₄)(OH) ₆	0.04	0.04	0.03
Zircon	ZrSiO ₄	0.01	0.05	0.03
Thorite	ThSiO ₄	0.04	0.02	0.02
Titanite	CaTiSiO ₅	0.01	0.04	0.01
Pyrochlore	(Ca,Na) ₂ Nb ₂ O ₆ (OH,F)	0.02	0.03	0.01
Sphalerite	ZnS	0.02	0.02	0.02
Chervetite	Pb ₂ V ₂ O ₇	0.01	0.01	0.02
Xenotime	YPO ₄	P	0.01	P

P – mineral present, but found at less than 0.01%

ND – mineral not detected

SUMMARY AND CONCLUSIONS

The beneficiation of rare earth oxides was studied to find a collector that increased the grade and recovery of rare earths while rejecting gangue minerals. An optimal particle size, mineral composition, and liberation were accomplished through mineralogical studies. The P_{80} of the bastnaesite ore was calculated to be 50 μm for all the flotation studies. Microflotation was used to narrow the 19 candidate collectors to the three top performing collectors: collector 2, collector 5, and collector 8. Design of experiment was used to determine the significant variables and interactions. Collector 2 was evaluated to be the best collector; collector 8 and 14 both showed promise as potential replacements for fatty acid, also. There is potential to optimize each flotation scheme for all the novel collectors based on limited flotation experiments done per collector. Only rougher flotation was studied so the effect of how the collector would perform in cleaner or scavenger flotation circuits is unknown.

ACKNOWLEDGEMENTS

This research is supported by the Critical Materials Institute, an Energy Innovation Hub funded by the U.S. Department of Energy, Office of Energy Efficiency and Renewable Energy, and the Advanced manufacturing Office. The authors would like to thank everybody in the Kroll Institute for Extractive Metallurgy the Colorado School of Mines for their advice and assistance during this project. The authors would also like to thank Ames Lab for providing the novel collectors.

REFERENCES

Anderson, C. D. (2015). *Improved understanding of rare earth surface chemistry and its application to froth flotation* (Doctoral thesis). Colorado School of Mines, Golden, CO.

Assis, S. M., Montenegro, L. C. M., & Peres, A. E. C. (1996). Utilisation of hydroxamates in minerals froth flotation. *Minerals Engineering*, 9(1), 103–114. [https://doi.org/10.1016/0892-6875\(95\)00134-4](https://doi.org/10.1016/0892-6875(95)00134-4)

Gupta, C. K., & Krishnamurthy, (2005). *Extractive metallurgy of rare earths*. Boca Raton, FL: CRC Press.

Jordens, A., Marion, C., Kuzmina, O., & Waters, K. E. (2014). Surface chemistry considerations in the flotation of bastnäsite. *Minerals Engineering*, 66–68, 119–129 <https://doi.org/10.1016/j.mineng.2014.04.013>

Pradip (1981). *The surface properties and flotation of rare-earth minerals* (Doctoral thesis). University of California, Berkeley, Berkeley, CA.

Pradip, & Fuerstenau, D. W. (1983). The adsorption of hydroxamate on semi-soluble minerals. Part I: Adsorption on barite, calcite and bastnaesite. *Colloids and Surfaces*, 8(2), 103–119. [https://doi.org/10.1016/0166-6622\(83\)80079-1](https://doi.org/10.1016/0166-6622(83)80079-1)

Pradip, & Fuerstenau, D. W. (1985). Adsorption of hydroxamate collectors on semisoluble minerals Part II: Effect of temperature on adsorption. *Colloids and Surfaces*, 15, 137–146. [https://doi.org/10.1016/0166-6622\(85\)80061-5](https://doi.org/10.1016/0166-6622(85)80061-5)

U.S. Geological Survey (2017). *Mineral commodity summaries 2017*. <https://doi.org/10.313/70180197>